

## Solid Phase Extraction of Celecoxib from Drug Matrix and Biological Fluids by Grafted Poly $\beta$ -cyclodextrine/allyl Amine Magnetic Nano-particles

Sahar Kamari, Homayon Ahmad Panahi<sup>†</sup>, Nasim Baimani\* and Elham Moniri\*\*

*Department of Chemistry, Islamic Azad University, Central Tehran Branch, Tehran, Iran*

*\*Department of Chemistry, Islamic Azad University, Research and Science Branch, Tehran, Iran*

*\*\*Department of Chemistry, Varamin (Pishva) Branch, Islamic Azad University, Varamin, Iran*

(Received 7 October 2016; Received in revised form 16 February 2017; accepted 22 February 2017)

**Abstract** – Using nanotechnology, magnetic nanoparticles of iron oxide were produced via co-precipitation method and followed modification with organic compounds. In the next step, functionalized monomer was provided via coupling  $\beta$ -cyclodextrine and allylamine onto modified magnetic nanoparticles. These nanoparticles were used to establish the adsorption rate of celecoxib. Magnetic nanoparticles are modified by (3-mercaptopropyl)trimethoxysilane. Nano-adsorbent was characterized by analytical and spectroscopic methods, such as Fourier transform infrared spectroscopy, elemental analysis, thermo-gravimetric analysis, and transmission electron microscopy (TEM). Laboratory parameters, such as the kinetics of adsorption isotherms, pH, reaction temperature and capacity were optimized. Finally, by using this nano-adsorbent in the optimized condition, extraction of celecoxib from biological samples as urine, drug matrix and blood plasma was carried out by high performance liquid chromatography with sensitivity and high accuracy.

Key words: Celecoxib, Drug delivery, Magnetic nanoparticles, Solid phase extraction, Biological samples

### 1. Introduction

Celecoxib is a cox-2 class of anti-inflammatory compound with few gastric side effects. The HPLC analysis data of celecoxib are reported in the literature [1]. The metabolites of celecoxib have been characterized by LC-MS-MS and reported in the literature [2]. Celecoxib is a high lipophilic, poor soluble drug with oral bioavailability between 22% and 40% by conventional capsule dosage form [3]. It is evenly distributed in vivo and has a distribution volume of  $455 \pm 166$  L in humans [4]. This larger volume of distribution and low aqueous solubility may be related to the lipophilic nature of celecoxib and be reflective of low bioavailability. Celecoxib is extensively metabolized in humans and is excreted primarily as metabolites [3]. Many formulations have been attempted to improve its bioavailability by using various solvent systems [5], complexation with  $\beta$ -cyclodextrins [6,7], solid dispersions [8], manipulation of the solid state of the drug [9,10], development of floating celecoxib capsule [11], and using silica-lipid hybrid microcapsules [12]. Niosomes are unilamellar or multilamellar vesicles made up of nonionic surfactant and can entrap amphiphilic and hydrophobic solutes [13,14]. Niosomes have shown advantages as drug carriers, such as being a cheap and chemically stable alternative to liposomes, but they are associated with problems related to physical stability, such as fusion, aggregation, sedimentation, and leakage on storage [15]. Proniosomes, which are more stable during steriliza-

tion and storage [16], minimize these problems by using dry, free-flowing particles that immediately form niosomal dispersion when in contact with water. Proniosomes are suitable for administration by oral or other routes [17]. Preliminary studies indicate that niosomes may increase the adsorption of certain drugs from the gastrointestinal tract following oral ingestion and prolong the existence of the drug in systemic circulation [13]. The encapsulation of celecoxib in lipophilic vesicular structure may be expected to enhance the oral absorption and prolong the existence of the drug in systemic circulation of the drug due to the slow release of the encapsulated drug. Accordingly, our objective of this study was to prepare celecoxib proniosomes and evaluate the influence of pronio-somal formulation on its oral bioavailability in healthy human volunteers.

In the last decade there has been a spectacular development of magnetic nano-particles (MNPs) for biomedical applications, such as magnetic carriers for drug delivery aided by external magnetic fields, magnetic resonance imaging contrast agents or cancer therapy compounds for hyperthermia, among others [18-20]. More recently, new multifunctional magnetic nanoparticles capable of carrying out simultaneously a dual function, cancer diagnosis and therapy, have been under investigation. Magnetic nanoparticles for biomedical applications are usually formed by a mineral core of a magnetic element, such as iron, nickel, cobalt and their oxides, and an organic coating, such as dextran, polyethyleneglycol, poly(vinylpyrrolidone), streptavidin, poly-L-lysine, polyethylene imide [21-26]. Polymeric sorbents are mostly used for pollution [26,27]. The sorbents have high toxicity and so they contaminate the environment and also cannot be used for biological purpose. Due to the lower toxicity of iron oxides, the most commonly employed MNPs for biomedical applications

<sup>†</sup>To whom correspondence should be addressed.

E-mail: h.ahmadpanahi@iauctb.ac.ir

This is an Open-Access article distributed under the terms of the Creative Commons Attribution Non-Commercial License (<http://creativecommons.org/licenses/by-nc/3.0>) which permits unrestricted non-commercial use, distribution, and reproduction in any medium, provided the original work is properly cited.

have a magnetite core. The MNP physicochemical properties such as particle size, shape, hydrophilic nature, coating and surface charge will determine, to a great extent, biodistribution and biocompatibility [29-31]. Our purpose was to investigate the possibility of using grafted magnetic nanoparticle for the extraction of celecoxib from biological human fluids. Furthermore, a kinetic study for releasing of the drug in simulated gastric and intestinal fluids was demonstrated.

## 2. Experimental

### 2-1. Instruments

Infrared spectra were to be registered on a Jasco Fourier transform infrared spectrometer (FT-IR-410, Jasco Inc., Easton, Maryland, USA). The transmission electron microscopy (TEM) micrographs were obtained on a TEM-PHILIPS CM30 transmission electron microscopy, respectively. Ultraviolet-visible (UV-Vis) spectroscopy was obtained by Jasco Inc. (Tokyo, Japan) V-530 UV-Vis spectroscope.

Elemental analysis was by a PerkinElmer 2400 series II and thermogravimetric analysis was experimented by Linseis (Munich, Germany) model Vario EA cube elemental analyzer and TGA-50H (Shimadzu Corporation, Kyoto, Japan), respectively.

### 2-2. Reagents and Solutions

Anhydrous 1,4-Dioxane, 2,2' azobisisobutyronitrile (AIBN), (3-mercaptopropyl)trimethoxysilane, acetonitrile, acetic acid, acetone, tosyl chloride,  $\beta$ -cyclodextrine ( $\beta$ -CD), ethanol, trifluoroacetic acid (TFA) methanol and allylamine were purchased from Merck (Darmstadt, Germany). Other reagents were of analytical grade and used without any purification. Celecoxib was prepared from Tehran Daru Co. (Iran). The stock solution ( $100 \text{ mg L}^{-1}$ ) was prepared by solving  $0.005 \text{ g}$  celecoxib in  $50 \text{ mL}$  of methanol. Phosphate or acetate buffer ( $0.01 \text{ M}$ ) was used to control the pH of the solutions.

### 2-3. Coupling of $\beta$ -CD/allyl amine as functional monomer

Sodium hydroxide  $2 \text{ mL}$  ( $25\%$ ) was added gradually to  $\beta$ -CD ( $6 \text{ g}$ ) stirred in  $50 \text{ mL}$  distilled water. Solution of tosyl chloride ( $1 \text{ g}$ ) in acetonitrile was added to the above solution within  $45 \text{ min}$ . This solution was stirred for  $2 \text{ h}$  at room temperature. Then, HCl ( $1 \text{ M}$ ) was added to adjust the pH about 3. White color precipitation was then filtered. The resultant precipitation ( $2.23 \text{ g}$ ) and allyl amine ( $23 \text{ g}$ ) were refluxed for  $5 \text{ h}$ . The functional monomer was washed with methanol ( $30 \text{ mL}$ ) and acetonitrile ( $200 \text{ mL}$ ), then filtered and dried [32].

### 2-4. Polymer grafting

Magnetic nanoparticles (MNP) were synthesized by co-precipitation technique [33]. Grafting of polymerization onto magnetic nanoparticles involved using free-radical polymerization. Free-radical polymerization onto inorganic oxide support needs the surface to be modified. Bonding reactive functional sites such as organosilanes is used to modify the surface. A functional polymer should be grafted to the modified magnetic nanoparticles, which was performed using (3-

mercaptopropyl)trimethoxysilane. The modification was initiated by adding the  $5\%$  solution of (3-mercaptopropyl)trimethoxysilane in 1,4-dioxane to added  $3 \text{ g}$  magnetic nanoparticle and then refluxed for  $72 \text{ h}$ . The modified magnetic nanoparticles were washed by 1,4-dioxane and separated by magnet and dried in desiccators. The grafting of monomers onto modified magnetic nanoparticles was accomplished using a temperature controlled reactor. The reaction was performed under the condition of vigorous stirring and nitrogen atmosphere. Ethanol ( $20 \text{ mL}$ ) as solvent,  $\beta$ -CD/allyl amine ( $1.1 \text{ g}$ ) as functional monomer, AIBN ( $0.06 \text{ g}$ ) as initiator were used to prepare the degassed polymerization mixture. The modified magnetic nanoparticles were settled into the degassed polymerization mixture for  $7 \text{ h}$  at  $70^\circ\text{C}$ . Then,  $\beta$ -CD-containing polymer grafted magnetic nanoparticles (CCPG-MNP) were separated by magnetic force. Washing by ethanol was used as an efficient way to remove any contingent adsorbed homopolymers. Polymerization policy is illustrated in Fig. 1. The synthesized CCPG-MNP was characterized by FT-IR, elemental analysis, TGA, TEM and CHN.

### 2-5. HPLC System

Agilent HPLC, 1200 series, used for chromatographic separations, was equipped with a UV/Vis detector. Separations were performed on a Zorbax Extend C18 column ( $25 \text{ cm} \times 4.6 \text{ mm}$ , with  $3 \text{ mm}$  particle size) from the Agilent Company (Wilmington, DE, USA). The mixture of acetonitrile and phosphate buffer  $0.01 \text{ M}$  ( $\text{pH} = 4.8$ ) ( $45:55 \text{ v/v}$ ), at a flow rate of  $1.2 \text{ mL min}^{-1}$  took part as mobile phase in isocratic elution mode in HPLC system. The injection volume was  $10 \mu\text{L}$  for all samples. The detection was performed at a wavelength of  $252 \text{ nm}$  and ambient temperature.

### 2-6. Batch method of celecoxib adsorption/desorption

A set of solutions ( $1 \text{ mL}$ ) containing  $2 \mu\text{g mL}^{-1}$  of celecoxib was placed in a micro-test tube, and their pH levels adapted to 6 using a buffer solution. After addition of CCPG-MNP ( $0.01 \text{ g}$ ) to each solution, the mixture was vortexed for  $60 \text{ min}$ . Then CCPG-MNP was separated magnetically, and the sorbed celecoxib was eluted with methanol/ACETIC ACID/TFA. HPLC was used to demonstrate the concentration of celecoxib in the eluent.

### 2-7. Isotherm studies

For a successful isotherm study, a series of test tubes containing  $10 \text{ mL}$  diluted solutions of celecoxib ( $2 \mu\text{g mL}^{-1}$ ) in acetate buffer ( $\text{pH}=6$ ) were prepared and  $0.05 \text{ g}$  of CCPG-MNP was added to them. The following equation was used to compute the amount of celecoxib at equilibrium  $q_e$  ( $\text{mg g}^{-1}$ ) on CCPG-MNP:

$$q_e = (C_0 - C_e) V / W \quad (1)$$

where  $C_0$  and  $C_e$  ( $\text{mg L}^{-1}$ ) are initial and equilibrium concentrations of celecoxib, respectively,  $V$  ( $\text{L}$ ) is the volume of the solution, and  $W$  ( $\text{g}$ ) is the mass of the CCPG-MNP.

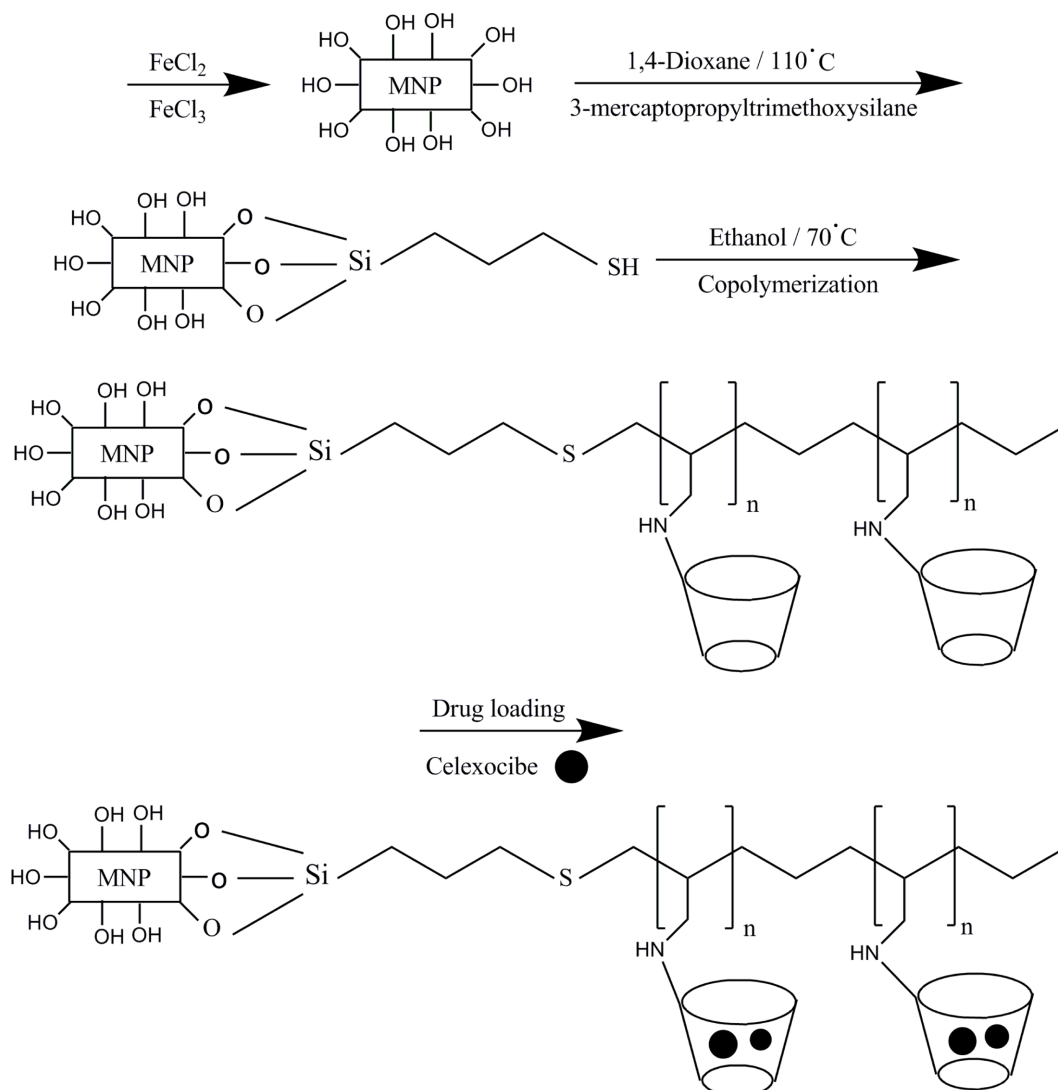


Fig. 1. Schematic of synthesizing CCPG-MNP.

### 2-8. In vitro drug release

The release profiles of celecoxib were studied using simulated gastric fluid (pH 1.2) and simulated intestinal fluid (pH 7.4). The release of celecoxib in enteric fluids was investigated in shaking and without shaking mode at  $37^\circ\text{C}$ . The celecoxib amount of samples in predefined time intervals was measured by HPLC.

## 3. Results and Discussion

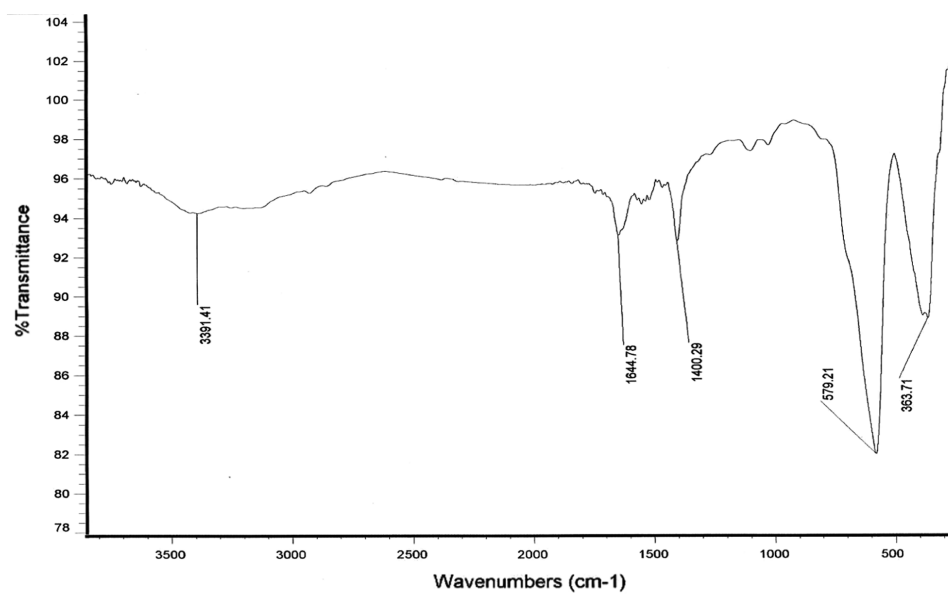
### 3-1. Characterization

Fe-O stretching band and O-H stretching peak were at  $579\text{ cm}^{-1}$  and  $3391\text{ cm}^{-1}$  in FT-IR spectrum of MNP, respectively. Peaks revealed at  $2919\text{ cm}^{-1}$  and  $1546\text{ cm}^{-1}$  are related to C-H stretching and  $\text{CH}_2$  stretching in (3-mercaptopropyl)trimethoxysilane-magnetic nanoparticles, respectively. Existence of C-H groups after modification indicates successful immobilization method. CCPG-MNP spectrum indicates the extra peaks related to C-O, C=O, and hydroxyl groups, at  $1148$ ,  $1693$  and  $3669\text{ cm}^{-1}$ , respectively (see Fig. 2). Existence of the expected groups in the different steps of CCPG-MNP synthesis

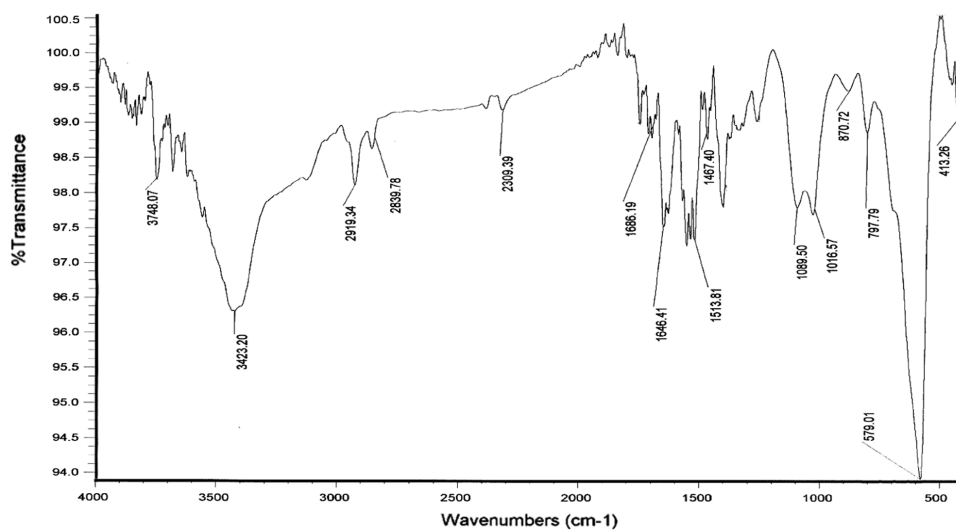
was verified by the revealed peaks at different positions in FT-IR spectrum. CCPG-MNP was also characterized by elemental analysis. Percentage of carbon, nitrogen and hydrogen in CCPG-MNP was 4.29, 0.96 and 1.15, respectively. The existence of carbon and nitrogen in CCPG-MNP confirmed that polymeric groups containing nitrogen and carbon were grafted onto nano-iron oxide. Thermogravimetric analysis (Fig. 3) was used to determine the thermal behavior of magnetic-nanoparticles and compared with CCPG-MNP. The weight of the nanoparticles was reduced about 4.0% up to  $600^\circ\text{C}$  due to the removal of adsorbed water (1.2%) and water in the crystal structure (2.8%) in magnetic nanoparticles. In the same situation, CCPG-MNP showed 14% weight loss up to  $600^\circ\text{C}$ . In other words, 9% of weight loss was due to the decomposition of polymer chains grafted to inorganic oxide nanoparticles. The particle size of the nanoparticles was in range of 30~80 nm in diameter and they were spherical. TEM images verify that in Fig. 4.

### 3-2. Optimization of parameters

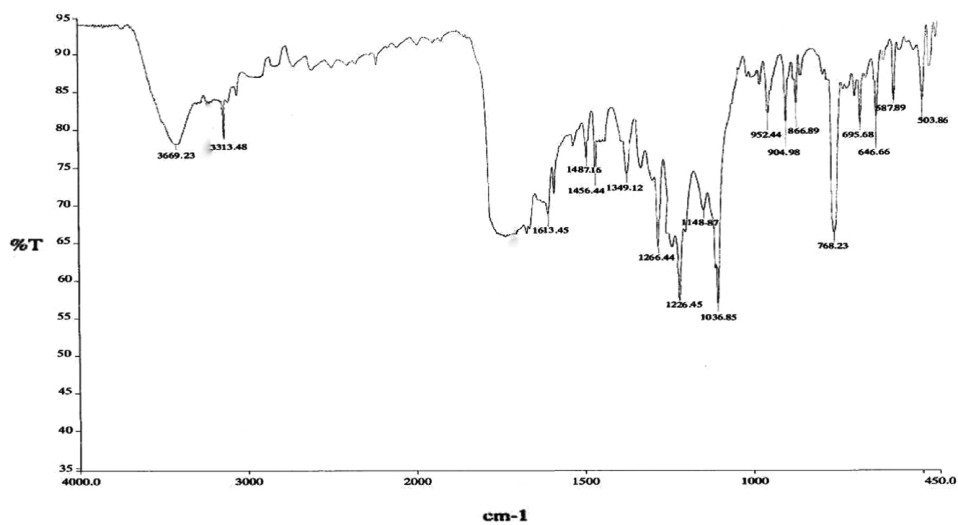
The degree of celecoxib sorption at different pH values (3.5~7.5)



(a)



(b)



(c)

Fig. 2. FT-IR spectrum of MNP (a), modified MNP (b) and CCPG-MNP (c).

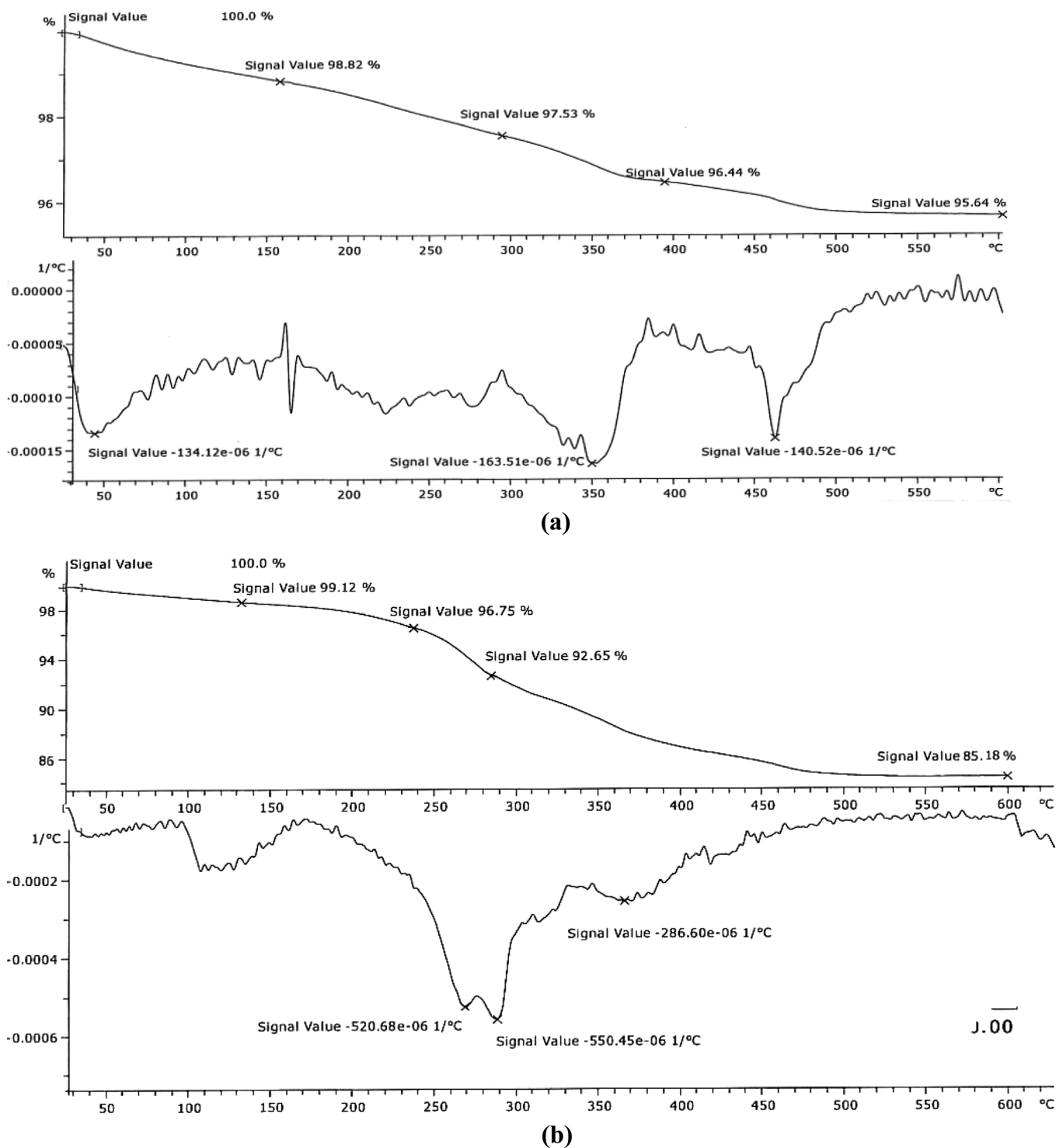


Fig. 3. TGA thermogram of MNP (a) and CCPG-MNP (b).

was determined using batch method. Optimum pH was observed at 6 (Fig. 5). Since the celecoxib is classified in neutral drug, the best electrostatic force between CCPG-MNP and desired drug was observed in the moderate acidic pH. The pH of greater than 7.5 was not experimented because of the dissolution of the magnetic nanoparticles in alkaline pH. Fig. 6 illustrates the kinetic sorption of celecoxib at pH 6. A sufficient time for complete sorption of celecoxib is about 1 h.

The half-time of the saturation sorption was 5 min. In other experiment, various eluents composed of methanol, acetic acid and TFA with different percentage were used to test the best extraction recovery of celecoxib. The result is listed in Table 1 and methanol was selected as the best eluent. Temperature effect on sorption of celecoxib by CCPG-MNP at pH 6 is presented in Fig. 7. As temperature increases above 20 °C, the sorption of celecoxib by CCPG-MNP decreases.

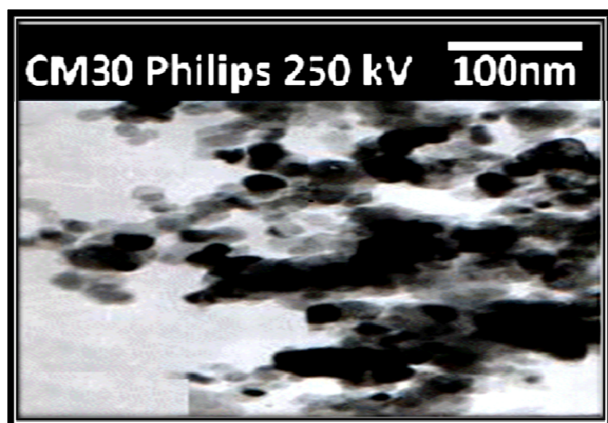


Fig. 4. TEM images of CCPG-MNP.

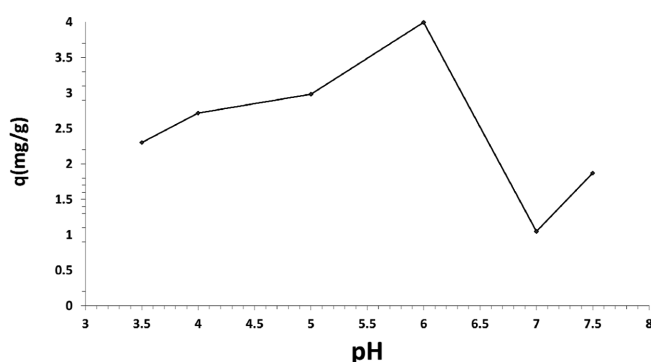


Fig. 5. Effect of pH on sorption of celecoxib onto CCPG-MNP. Volume of each 1 mL containing  $20 \mu\text{g mL}^{-1}$  of celecoxib. Their pH values were adjusted with buffer solutions. The 0.01 g of CCPG-MNP was added to each solution and the mixture was shaken for 30 min.

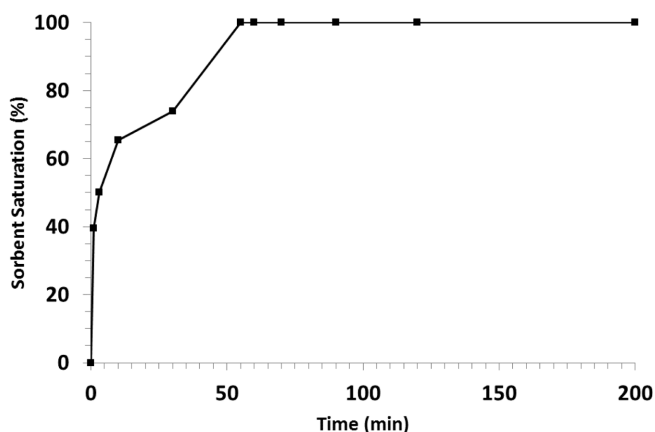


Fig. 6. Kinetics of celecoxib sorption on CCPG-MNP.

This probably could be caused by the increased molecular movements with temperature increase.

### 3-3. Adsorption isotherms

Adsorption isotherm was used to represent the amount of celecoxib adsorbed per unit of CCPG-MNP. It was evaluated for optimized celecoxib removal in equilibrium concentration at  $20^\circ\text{C}$ . Langmuir, Freundlich, Temkin and Redlich-Peterson were used as isotherm models for celecoxib sorption.

Korean Chem. Eng. Res., Vol. 55, No. 3, June, 2017

Table 1. Evaluation of recovery in different eluent

Eluent	Recovery (%)
MeOH	92
MeOH/AA (98:1)	69
MeOH/TFA (99:1)	84
MeOH/TFA/AA (98:1:1)	66
MeOH/TFA/AA (94:1:5)	56

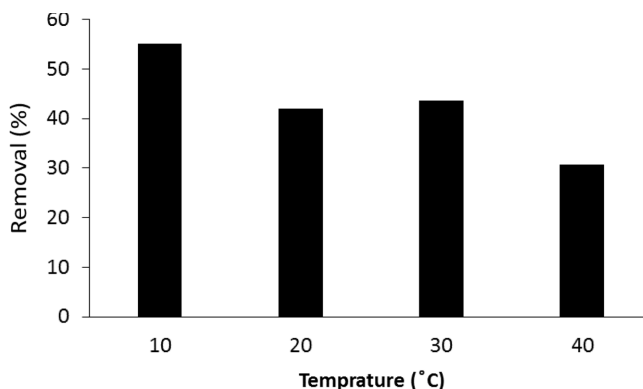


Fig. 7. Effect of temperature on sorption of celecoxib onto CCPG-MNP.

Langmuir equation is given by [34]:

$$C_e/q_e = (1/q_{max}K_L) + (C_e/q_{max})$$

where  $q_{max}$  is the maximum celecoxib sorption capacity corresponding to complete monolayer coverage on CCPG-MNP surface ( $\text{mg g}^{-1}$ ), and  $K_L$  is the Langmuir constant ( $\text{L mg}^{-1}$ ). The calculated Langmuir parameters using the Eq. (2) are listed in Table 2. Langmuir equation characteristics can be expressed by a dimensionless separation factor,  $R_L$ , defined by  $R_L = 1/(1 + K_L C_0)$ .

Hall *et al.* [35]. discuss that  $R_L$  values can divide the adsorption nature into four different ranges, including irreversible ( $R_L=0$ ), favorable ( $0 < R_L < 1$ ), linear ( $R_L=1$ ) and unfavorable ( $R_L > 1$ ). According to Table 2, the value of  $R_L$  (0.03) is in the favorable sorption range.

The Freundlich is an experimental isotherm applied to define heterogeneous systems in which it is specified by the heterogeneity factor  $1/n$  with the equation [36]:

$$\ln q_e = \ln K_F + 1/n (\ln C_e)$$

where  $K_F$  is the Freundlich constant ( $\text{mg g}^{-1}$ ) ( $\text{L mg}^{-1}$ )<sup>1/n</sup>. The experimental guide of this model is based on adsorption on a heterogeneous modified surface. It is supposed in the Freundlich isotherm that increase in the fraction of occupied active site would reduce logarithmically the enthalpy of adsorption. It can be deduced that the Freundlich isotherm predicts that the celecoxib concentration on CCPG-MNP will increase since the celecoxib concentration in the solution increases.

The Temkin equation indicates a decrease of sorption energy corresponding to increase of the degree of completion of the sorptional centers of CCPG-MNP [37]

$$q_e = B \ln A + B \ln C_e$$

**Table 2. Isotherm parameters obtained by using linear method**

Langmuir isotherm model				
Temperature (°C)	$q_{max}$ (mg/g)	$K_L$ (L/mg)	$R_L$	$R^2$
20	2.2	1.1	0.03	0.9988
Freundlich isotherm model				
Temperature (°C)	$K_F$ (mg/g) (L/mg) <sup>1/n</sup>	n	$R^2$	
20	0.89	2.90	0.9008	
Temkin isotherm model				
Temperature (°C)	A (L/g)	B	b(J/mol)	$R^2$
20	21.93	0.36	6830	0.9383
Redlich–Peterson isotherm model				
g	B (dm <sup>3</sup> /mg) <sup>B</sup>	A(dm <sup>3</sup> /g)	$R^2$	
0.986	1.72	3.3	0.9909	

where  $B=RT/b$  and  $b$  is the Temkin constant related to heat of celecoxib sorption ( $J mol^{-1}$ ).  $R$  is the gas constant ( $8.314 J mol^{-1} K^{-1}$ ),  $T$  is the absolute temperature (K) and  $A$  is the Temkin isotherm constant ( $L g^{-1}$ ). Temkin isotherm constants are listed in Table 2.

The Redlich-Peterson isotherm is characterized by three constants,  $A$ ,  $B$  and  $g$  ( $0 < g < 1$ ), and unifies the features of Langmuir and Freundlich isotherms [38]

$$\ln(A(C_e/q_e) - 1) = g \ln C_e + \ln B$$

The Redlich-Peterson isotherm parameters for the sorption of celecoxib onto CCPG-MNP using linear regression are listed in Table 2. The measured results show that the value of  $g$  is close to 1, which indicates the isotherms are approaching the Langmuir model.

### 3-4. Method application

To verify the reliability and suitability of the proposed procedure for the determination of celecoxib in different real samples, celecoxib was extracted from human biological fluids and pharmaceutical samples using the developed solid phase extraction technique. Sampling of human serum and urine was carried out without any pre-treatments. The extractions were performed at optimum conditions. Red blood cells were separated from human blood by centrifugation at  $4700 \times g$  for 25 min at room temperature, then filtered and frozen at  $-20^\circ C$  before use. HBS antigen, HCV (Hepatitis C) and HIV I, II antibodies were all negative for the human blood. The consequences, listed in Table 3, represent a good recovery in human urine, pharma-

ceutical samples and poor recovery in human serum. The recovery was calculated as the amount of the total celecoxib which was extracted into the CCPG-MNP and subsequently into eluent. The poor recovery in human serum may be due to the blockage of binding sites on the CCPG-MNP by serum components or a rather strong competition of serum components for celecoxib binding. Good recovery in human urine and pharmaceutical samples verifies the efficiency of CCPG-MNP in celecoxib extraction.

### 3-5. Analytical approach

The linearity and accuracy for celecoxib in the proposed method are listed in Table 4. Calibration curves were obtained by spiked standards at various celecoxib concentrations under the optimized sorption condition. The limit of detection and limit of quantification corresponding to three and ten times the blank standard deviations are presented in Table 4, too. The repeatability and reproducibility of the method were verified by the relative standard deviation (RSDs) for four replicate designations of the sample at a  $2 \mu g mL^{-1}$  level of celecoxib in one day and on three different days (four times a day), respectively. Since the RSDs (less than 3%) and  $R^2$  value of the developed method (0.9997) are satisfactory, it is obvious that the proposed method was carried out well for CCPG-MNP, analytically.

### 3-6. Celecoxib release

Celecoxib release by CCPG-MNP in simulated intestinal fluid (pH 7.4) and simulated gastric fluid (pH 1.2) are depicted in Fig. 8 and Fig. 9, respectively. Nearly 96% of the celecoxib was released in

**Table 3. Determination of celecoxib in different samples**

Sample	Concentration of celecoxib ( $\mu g mL^{-1}$ )	Added ( $\mu g mL^{-1}$ )	Found* ( $\mu g mL^{-1}$ )	Recovery (%)
Plasma	-	0.50	$0.19 \pm 0.10$	38.1
Urine	-	0.50	$0.52 \pm 0.08$	104.0
Tablet	2.00	-	$1.98 \pm 0.13$	99.1

\*For three determinations

**Table 4. Analytical performance of celecoxib determination**

Analytical calibration curve	R <sup>2</sup>	Linear range ( $\mu g L^{-1}$ )	RSD*		LOD ( $ng mL^{-1}$ )	LOQ ( $ng mL^{-1}$ )
			Repeatability	Reproducibility		
$Y=0.0607X+0.001$	0.9997	0.5~40	1.21	1.51	5	18

\*For four experiments

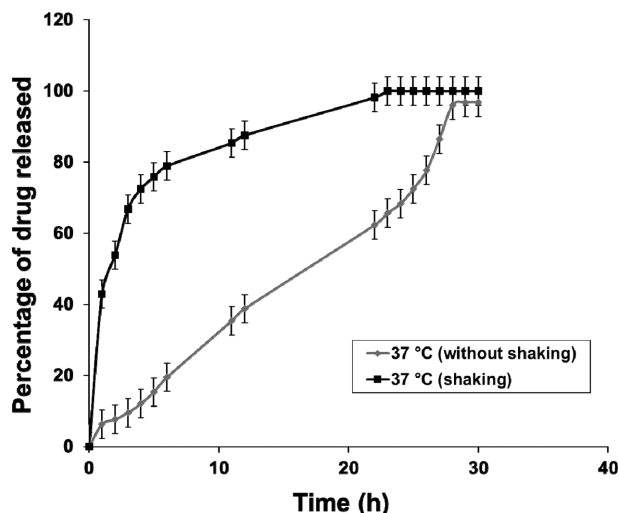


Fig. 8. Celexocib release profile in simulated intestinal fluid (pH 7.4).

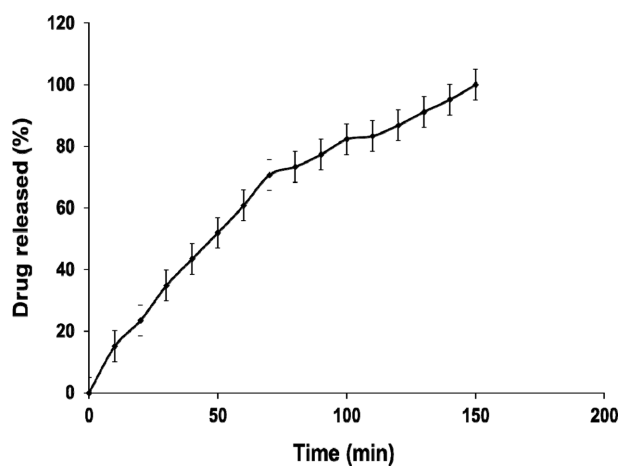


Fig. 9. Celexocib release profile in simulated gastric fluid (pH 1.2).

the simulated intestinal fluid with a steep slope in 5 h and then with steady slope over a period of 30 h at 37 °C. However, in the simulated gastric fluid, about 50% of celecoxib with a steep slope was released in about 1 h at 37 °C, thereafter, nearly 100% of celecoxib with a gentle slope released until 150 min. Thus, celecoxib was released better in the simulated gastric fluid due to the existence of high acetic media.

#### 4. Conclusions

A new polymer grafted magnetic nano-particle was developed for the extraction of celecoxib and then characterized by HPLC determination. Experimental results show that the proposed approach has some advantages, including simplicity, efficiency of extraction and little solvent consumption. The adsorption isotherm study indicated that the adsorption of celecoxib by CCPG-MNP follows the Langmuir isotherm model better than the other isotherm models. As Langmuir isotherm analysis shows, the monolayer adsorption capacity was obtained to be 2.2 mg g<sup>-1</sup> at 20 °C. The pharmaceutical and biologi-

cal samples recovery values represented that the adsorption of celecoxib by CCPG-MNP had satisfactory results.

#### References

- Sreenivasu, M. K., Narayana, C. L., Sreenivas Rao, D. and Om, R. G., *J. Pharm. Biomed. Anal.*, **22**, 949 (2000).
- Zhang, J. Y., Wang, Y., Dudkowski, C., Yang, D., Chang, M., Yuan, J., Paulson, S. K. and Breau, A. P., *J. Mass Spectrom.* **35**, 1259 (2000).
- Paulson, S. K., Hribar, J. D., Liu, N. W., Hajdu, E. J., Bible, R. H. and Piergies, A., *Drug Metab. Dispos.*, **28**, 308 (2000).
- Paulson, S. K., Vaughn, M. B., Jessen, S. M., Lawal, Y., Gresk, C. J. and Yan, B., *J. Pharmacol. Exp. Ther.*, **297**(2), 638 (2001).
- Neelam, S. and Sonu, B., *AAPS Pharm. Sci. Tech.*, **4**(3), 33 (2003).
- Narender, R., Tasneem, R., Ramakrishna, S., Chowdary, K. and Prakash, V., *AAPS Pharm. Sci. Tech.*, **6**(1), 7 (2004).
- Nagarsenker, M. S. and Joshi, M. S., *Drug. Dev. Ind. Pharm.* **31**(2), 169 (2005).
- Dixit, R. and Nagarsenker, M., *Indian. J. Pharm. Sci.*, **69**(3), 370 (2007).
- Gupta, V. R., Mutalik, S., Patel, M. M. and Jani, G. K., *Acta Pharm.* **57**(2), 173 (2007).
- Guzman, H. R., Tawa, M., Zhang, Z., Ratanabanangkoon, P., Shaw, P. and Gardner, C. R., *J. Pharm. Sci.*, **96**(10), 2686 (2007).
- Javed, A., Shweta, A., Alka, A., Anil, K., Rakesh, K. and Roop, K., *AAPS Pharm. Sci. Tech.*, **8**(4), Article 119 (2007).
- Angel, T., Spomenka, S., Andrew, K., Thomas, R. and Clive, A., *J. Control Release* **134**, 62 (2009).
- Azmin, M. N., Florence, A. T., Handjani-Vila, R. M., Stuart, F. B., Vanlerberghe, G. and Whittaker, J. S., *J. Pharm. Pharmacol.* **37**, 237 (1985).
- Baillie, A. J., Florence, A. T., Hume, L. R., Muirhead, G. T. and Rogerson, A., *J. Pharm. Pharmacol.*, **37**, 863 (1985).
- Namdeo, A. and Jain, N. K., *J. Microencapsul.* **16**, 731 (1999).
- Blazek-Welsh, A. I. and Rhodes, D. G., *Pharm. Res.*, **18**, 656 (2001).
- Hu, C. and Rhodes, D. G., *Int. J. Pharm.*, **185**, 23 (1990).
- Huang, J., Zhong, X., Wang, L., Yang, L. and Mao, H., *Theranostics*, **2**, 86 (2012).
- Pankhurst, Q. A., Thanh, N. K.T., Jones, S. K. and Dobson, J., *J. Phys. D Appl. Phys.*, **42**, 224001 (2009).
- Wang, M. and Thanou, M., *Pharmacol. Res.*, **62**, 90 (2010).
- Lee, D. E., Koo, H., Sun, I. C., Ryu, J. H., Kim, K. and Kwon, I. C., *Chem. Soc. Rev.*, **41**, 2656 (2012).
- Shubayev, V. I., Pisanic Ii, T. R. and Jin, S., *Adv. Drug. Deliv. Rev.*, **61**, 467 (2009).
- Pan, B., Cui, D., Sheng, Y., Ozkan, C., Gao, F. and He, R., *Cancer Res.*, **67**, 8156 (2007).
- Qi, L., Wu, L., Zheng, S., Wang, Y., Fu, H. and Cui, D., *Bio-macromol.*, **13**, 2723 (2012).
- Ruan, J., Wang, K., Song, H., Xu, X., Ji, J. and Cui, D., *Nanoscale. Res. Lett.*, **6**, 1 (2011).
- Nezhati, M. N., Panahi, H. A., Moniri, E., Kelahrodi, S. R., Assadian, F. and Karim, M., *Korean J. Chem. Eng.* **27**(4), 1269 (2010).
- Panahi, H. A., Sharif, A. A. M., Bigonah, M., Moniri, E., *Korean J. Chem. Eng.*, **26**(6), 1723 (2009).



28. Cole, A. J., David, A. E., Wang, J., Galbán, C. J., Hill, H. L. and Yang, V. C., *Biomaterials* **32**, 2183 (2011).
29. Gupta, A. K. and Gupta, M., *Biomaterials* **26**, 3995 (2005).
30. Gupta, A. K., Naregalkar, R. R., Vaidya, V. D. and Gupta, M., *Nanomedicine* **2**, 23 (2007).
31. Villanueva, A., Cañete, M., Roca, A. G., Calero, M., Veintemillas-Verdaguer, S. and Serna, C. J., *Nanotechnol.*, **20**, 115103 (2009).
32. Ye, Y., Sun, Y., Zhao, H., Lan, M., Gao, F., Song, C., Lou, K., Li, H. and Wang, W. *Int. J. Pharm.* **458**, 110 (2013).
33. Mahdavian, A. R. and Mirrahimi, M. S., *Chem. Eng. J.*, **159**, 264 (2010).
34. Langmuir, I., *J. Am. Chem. Soc.*, **40**, 1361 (1918).
35. Hall, K. L., Eagleton, L. C., Acrivos, A. and Vermeulen, T., *Ind. Eng. Chem. Fundam.*, **5**, 212 (1966).
36. Freundlich, H. M., *J. Phys. Chem.*, **57**, 385 (1906).
37. Temkin, M. I. and Pyzhev, V. *Acta Physiochim.*, **12**, 327 (1940).
38. Redlich, O. and Peterson, D. L., *J. Phys. Chem.*, **63**, 1024 (1959).